Frontiers in Heat and Mass Transfer

Tech Science Press

https://doi.org/10.32604/fhmt.2026.083157

ARTICLE

Spray Parameter and Additive Concentration Effects on Smooth Surface Spray Cooling: From Flow Visualization to Nusselt Correlation

Dawar Asfandyar Khan, Yanyu Chen, Haokang Zhang and Yu Wang*

College of Urban Construction, Nanjing Tech University, Nanjing, China

*Corresponding Author: Yu Wang. Email: yu-wang@njtech.edu.cn

Received: 30 March 2026; Accepted: 08 May 2026; Published: 31 August 2026

ABSTRACT: Efficient thermal management of high heat flux systems is critical in modern electronic and energy devices. Spray cooling, with its high heat removal capability and uniform surface cooling, is widely recognized as an effective technique. Extensive studies have explored spray cooling using water and other working fluids, focusing on droplet dynamics, surface wetting, and heat transfer enhancement. However, the influence of low-concentration alcohol additives on spray cooling performance and evaporation dynamics remains insufficiently understood. This work systematically investigates the non-monotonic heat-transfer behaviour by varying spray height, flow rate, and heat input individually, focusing on the effects of low-concentration ethanol additives (2%, 4%, and 5%). A single-nozzle spray cooling system is used to compare the thermal performance of pure water and ethanol–water mixtures. Experiments are conducted at a constant spray pressure of 0.2 MPa, with spray height (1.22–2.89 cm), flow rate (0.5–0.75 L/min), and heating power (200–260 W) varied. Surface temperature evolution is monitored, and the transient heat transfer coefficient is calculated to characterize cooling performance. Results show that small amounts of ethanol significantly alter droplet evaporation, liquid spreading, and surface wetting, leading to distinct cooling responses compared to pure water. These findings enhance the understanding of low-concentration alcohol additives in spray cooling and provide guidance for improving heat dissipation in high-heat-flux systems. Future work should explore the coupling effects of droplet dynamics, surface microstructures, and alternative working fluids to optimize spray cooling efficiency.

KEYWORDS: Spray cooling; heat transfer; alcohol–water mixtures; battery thermal management; droplet impingement; correlation equation

1 Introduction

Efficient thermal management is a critical requirement in modern high-heat-flux applications, especially in power electronics and compact electronic devices, where increasing power density and miniaturization intensify heat dissipation challenges [1–3]. As device miniaturization continues and power densities increase, the available heat-dissipation area decreases, resulting in severe thermal loads that challenge conventional cooling techniques [4]. Traditional air cooling and single-phase liquid cooling methods are often inadequate under such conditions because of their limited heat removal capability and the large temperature gradients they produce. Consequently, advanced cooling strategies capable of maintaining stable surface temperatures under elevated heat fluxes have become an important focus of thermal-engineering research [5–7].

Among the various approaches proposed for high-heat-flux thermal management, spray cooling achieves high heat removal through droplet impingement, surface wetting, and phase-change mechanisms, resulting in relatively uniform surface temperature [8]. When a spray of fine droplets impacts a heated surface, multiple heat-transfer mechanisms may occur simultaneously, including droplet spreading, liquid-film formation, nucleate boiling, thin-film evaporation, and vapor generation at higher thermal loads [9]. The coupling of these processes enables spray cooling to achieve high heat-removal rates while maintaining relatively uniform surface temperatures and low coolant consumption [10]. These characteristics make spray cooling particularly promising for applications requiring compact and efficient thermal management.

The performance of spray-cooling systems depends strongly on operating conditions and working-fluid properties. Previous studies have demonstrated that heat transfer performance is strongly influenced by several factors, including nozzle geometry, spray height, flow rate, droplet size distribution, surface wettability, and imposed heat flux [11,12]. In addition to system-level parameters, modifying the working fluid has been investigated to improve atomization and surface wetting. Water is employed extensively because of its high latent heat, advantageous thermal characteristics, and accessibility [13]. Additives can change the fluid properties, such as surface tension and evaporation. Because they lower surface tension, encourage droplet breakdown, and improve liquid spreading on hot surfaces, ethanol–water combinations are particularly interesting [14,15]. Under some circumstances, this might improve surface coverage and cooling performance.

However, the influence of ethanol addition on spray-cooling heat transfer is complicated because it simultaneously alters several thermophysical properties, such as thermal conductivity, volatility, and latent heat. The summative effect on heat-transfer performance can thus be non-monotonic and highly dependent on operating conditions [16,17]. Although previous studies have explored ethanol–water mixtures in spray-cooling systems, further controlled experiments are required to clarify the cooling behavior of low-concentration ethanol additives as compared to pure water under well-defined conditions [18–20].

This paper presents a systematic study of low-concentration ethanol–water mixtures (2%–5% vol) on a smooth heated surface. By combining transient heat-transfer measurements with high-speed visualization, the study reveals how minimal alteration of fluid composition affects droplet spreading, evaporation, and spray-cooling heat transfer. Specifically, the experiments show the characteristics of the non-monoatomic behavior of droplets at the surface, which explain increased surface coverage and improved cooling performance at specific ethanol concentrations. Experiments were performed using a single-nozzle spray system at a constant spray pressure of 0.2 MPa, with spray heights of 1.22–2.89 cm, flow rates of 0.5–0.75 L/min, and heating powers of 200–260 W. Surface temperature measurements and transient heat-transfer coefficient (HTC) analysis were used to characterize cooling performance under these conditions.

The work aims to explain the influence of ethanol concentration on spray-cooling heat-transfer behavior and identify concentration-dependent performance differences. Although ethanol tends to cause a reduction in the surface tension and increase the spreading of the droplet, the resulting heat-transfer enhancement is not necessarily monotonic. In particular, the 5% vol ethanol mixture exhibits enhanced cooling as compared to the 2% vol and 4% vol mixtures, potentially because of a favorable balance of surface-tension reduction, droplet atomization, and evaporation dynamics, which enhances surface wetting and liquid-film renewal during spray impact. These findings provide new insight into the role of ethanol concentration in spray-cooling systems and contribute to improved thermal-management strategies for high-heat-flux applications.

2 Experiments & Data Processing

2.1 Experimental System

The spray-cooling apparatus used in this study comprised four integrated subsystems: a working-fluid delivery unit, a heating unit, a visualization unit, and a data-acquisition unit. A schematic representation of the experimental arrangement is shown in Fig. 1.

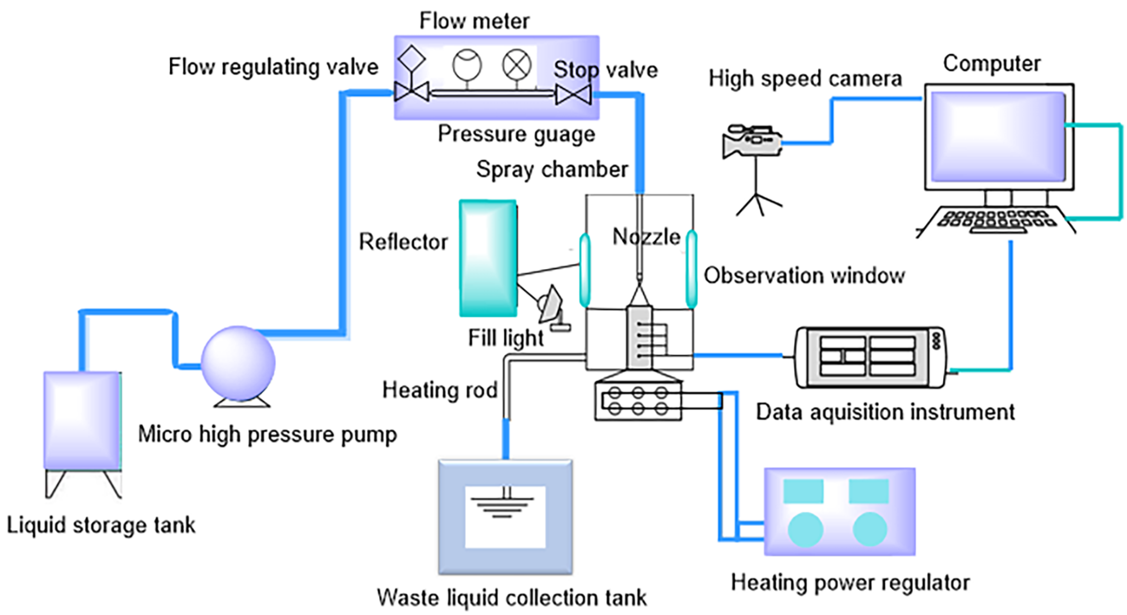

Figure 1: Schematic diagram of the spray cooling system.

The working-fluid delivery unit consisted of a liquid reservoir, a micro high-pressure pump, a flow-control valve, a flow meter, a pressure gauge, and a shut-off valve. During operation, the test fluid was pumped from the reservoir to the spray nozzle mounted inside the chamber, where it was atomized and directed onto the heated target surface. The spray pressure was maintained at a constant value of 0.2 MPa throughout all experiments.

The heated target was formed by the upper surface of a copper block used as the test substrate. The exposed circular heat-transfer area had a diameter of 2.4 cm, corresponding to an effective surface area of 4.52 cm^2. Heat was supplied to the copper block by an embedded electrical cartridge heater, and the input power was regulated using a programmable power controller. The applied heating power ranged from 200 to 260 W, corresponding to nominal heat fluxes of 44.25–57.52 W/cm^2 based on the exposed surface area. After impingement and heat exchange at the test surface, the discharged liquid was collected at the base of the spray chamber and transferred to a waste reservoir. All experiments were conducted under ambient atmospheric conditions.

Flow visualization was performed through a transparent observation window using a high-speed camera positioned in front of the chamber. Illumination was provided by an external light source in combination with a reflector to ensure sufficient image clarity for observing spray development, surface wetting behaviour, and vapor formation in the vicinity of the heated surface. Temperature signals and operating parameters were continuously acquired through a data-acquisition system and stored for subsequent analysis.

A single-fluid pressure nozzle with an orifice diameter of 1 mm was used for all tests. The working fluids examined in this study were pure water and ethanol–water mixtures containing 2%, 4%, and 5% vol ethanol. Pure water was selected as the reference fluid for evaluating the influence of low-concentration ethanol addition on spray-cooling performance.

2.2 Test Conditions and Operating Matrix

Experiments were performed at spray heights of 1.22–2.89 cm, volumetric flow rates of 0.5–0.75 L/min, and heating powers of 200–260 W, while the spray pressure was maintained constant at 0.2 MPa. The tested operating conditions are listed in Table 1.

Table 1: Tested operating conditions used in the spray-cooling experiments.

Parameter	**Range**
Spray height (cm)	1.22, 1.627, 2.17, 2.89
Flow rate (L/min)	0.50, 0.583, 0.667, 0.75
Heat input (W)	200, 220, 240, 260
Spray pressure (MPa)	0.2
Nominal heat flux (W/cm^2)	44.25, 48.67, 53.10, 57.52
Tested Fluids	Pure water, ethanol–water mixtures (2%, 4%, 5% vol)

In this study, each experimental case was designed to vary only one operating parameter at a time, either spray height, flow rate, or heat input, while keeping the others fixed. Therefore, the observed differences in cooling performance directly reflect the effect of the individual parameter under investigation. For each operating case, four working fluids were examined: pure water and ethanol–water mixtures containing 2%, 4%, and 5% vol ethanol. Cooling performance was assessed from the measured transient temperature response, the corresponding heat-transfer coefficients, and synchronized flow visualization. Accordingly, the experimental matrix was designed to provide a controlled comparative dataset for evaluating the effect of low-concentration ethanol addition on spray-cooling behaviour within the operating range of the present apparatus.

2.3 Temperature Measurements

Temperatures within the copper heating block were measured using embedded K-type armoured thermocouples installed at predetermined depths along the vertical centreline of the block. For heat-transfer analysis, the representative test-surface temperature was approximated by the average of thermocouples No. 4 and No. 5, which were positioned closest to the heated surface. The test-surface temperature was therefore defined as:

$$T_{test} = \frac{T_4 + T_5}{2} \tag{1}$$

where T_4 and T_5 are the temperatures recorded by thermocouples No. 4 and No. 5, respectively.

The working-fluid temperature was evaluated as the average of the inlet and outlet fluid temperatures:

$$T_f = \frac{T_{inlet} + T_{outlet}}{2} \tag{2}$$

The temperature difference driving convective heat transfer was then expressed as:

$$\triangle T = T_{test} - T_f \tag{3}$$

This temperature difference was used in the subsequent calculation of the convective heat-transfer coefficient.

2.4 Heat Flux and Heat-Transfer Coefficient Calculation

The surface heat flux (q'') was calculated from the electrical power supplied to the copper heating block:

$$q'' = \frac{Q}{A} = \frac{U \times I}{A} \tag{4}$$

where U is the applied voltage (V), I is the current (A), Q is the total heat supplied (W), and A is the exposed surface area of the copper heating block. In the present study, heat flux was initially expressed in W/cm^2 and later converted to W/m^2 for standard reporting using the relation 1 W/cm^2 = 10,000 W/m^2.

The convective heat transfer coefficient h was computed using the classical Newton's law of cooling:

$$h = \frac{q''}{\triangle T} \tag{5}$$

$$h = \frac{q''}{T_{test} - T_f} \tag{6}$$

where q'' is the surface heat flux, T_{test} is the representative surface temperature, and T_f is the average working-fluid temperature.

2.5 Spray Visualization and Performance Evaluation

High-speed visualization was employed to qualitatively examine spray behaviour under different operating conditions and working-fluid compositions. The recorded images were used to compare droplet dispersion, liquid-film development, surface wetting characteristics, and vapor formation in the vicinity of the heated surface.

These visual observations were used as supporting qualitative evidence for interpreting the measured thermal response. The visualization data were not treated as independent quantitative measurements and were therefore not used to derive spray parameters such as droplet size, impact velocity, or local film thickness.

The primary metric used to assess cooling performance was the heat-transfer coefficient obtained from the temperature-based analysis described above. Comparisons among the tested working fluids were carried out under identical operating conditions in order to evaluate the relative influence of ethanol concentration on spray-cooling behaviour within the present system.

3 Uncertainty Analysis

The uncertainties in the present spray-cooling experiments were evaluated using the error-propagation method proposed by Moffat [21]. Temperatures within the copper heating block were measured using embedded K-type armoured thermocouples, each with an individual uncertainty of ±0.8°C. The uncertainty in the calculated temperature gradient obtained from these thermocouples was estimated to be ±0.01. The working-fluid temperature at the spray outlet was measured using a PT100 platinum resistance thermometer with an accuracy of ±0.15°C. In addition, machining tolerances during laser drilling introduced a positional uncertainty of ±0.1 mm in thermocouple placement, which affected the geometric definition of the effective heating surface.

The uncertainties of the main derived parameters were estimated using the general uncertainty-propagation relation:

$$\delta R = \sqrt{\sum_i \left(\frac{\partial R}{\partial x_i}\partial x_i\right)^2} \tag{7}$$

where R represents the derived parameter, x_i denotes the directly measured variables, and δx_i represents their respective uncertainties. In the present study, the derived parameters included the surface heat flux (q''), the representative surface temperature T_{test}, and the heat-transfer coefficient (h).

Based on the uncertainty analysis, the estimated uncertainties were approximately ±1.1% for heat flux, ±0.57°C for surface temperature, and ±1.6% for the heat-transfer coefficient. These relatively small uncertainty levels indicate that the measurements were sufficiently precise for comparative spray-cooling analysis within the tested operating range.

All tests were performed at atmospheric conditions using a 1 mm single-fluid nozzle. Pure water and ethanol-water mixtures (2%, 4%, and 5% vol) were tested. Each experimental condition had only one operating parameter altered at a time, either spray height, flow rate, or heat input, with all the other parameters kept constant at a spray pressure of 0.2 MPa. Observed differences in heat-transfer performance are, therefore, the individual, but not the joint effect, of the parameter being varied. The ranges of tested parameters are summarized in Table 1.

4 Results and Discussion

This section provides experimental spray-cooling experiment results of pure water and ethanol–water mixtures (2%, 4%, and 5% vol). The cooling behavior within the tested operating window that was tested was compared using transient heat-transfer coefficient (HTC) data and flow visualization. Experiments were performed at atmospheric conditions using a single-fluid nozzle with a 1 mm orifice and a constant spray pressure of 0.2 MPa. Table 1 summarizes the ranges of tested parameters. Each experiment varied only one parameter at a time, spray height, flow rate, or heat input, while keeping the others constant. Observed variations in HTC are mainly due to the individual effect of the varied parameter, and visual data are used to explain the contribution of the spray dispersion, surface wetting, liquid replenishment, and vapor accumulation.

4.1 Flow Visualization and Characteristics under the Tested Operating Conditions

High-speed visualization was used to examine spray structure, surface wetting behavior, and vapor development under the tested operating conditions. Fig. 2 shows that, as thermal load increased, vapor generation near the impact region became progressively more pronounced, while the apparent liquid coverage at the surface center became less stable.

Fig. 2a shows a 200 W stable and transparent liquid layer on the heated surface, indicating effective wetting and sustained nucleate boiling. Droplet spreading was relatively uniform, while vapor generation remained limited, allowing continuous liquid–surface contact. This condition represents the reference flow regime in the present smooth-surface spray-cooling system. Fig. 2b 220 W shows that the spray impact area became wider, and vapor intensity increased near the center of impingement. The liquid film appeared less stable than in Fig. 2a, suggesting stronger evaporation and the early disruption of continuous rewetting. This image reflects the beginning of the transition from stable wetting to vapor-affected cooling. Fig. 2c 240 W shows the development of a thicker vapor layer above the heated surface, and the liquid–surface interaction became less distinct. Increased vapor generation reduced direct droplet contact with the wall and weakened the stability of the wetted region. This behavior indicates the onset of transition boiling, where vapor accumulation begins to limit cooling efficiency. Fig. 2d 260 W shows dense vapor clouds above the surface, indicating severe vapor accumulation and the beginning of local dry-out. The liquid film became highly unstable, and rewetting was significantly hindered by the vapor layer. Under this condition, the cooling mechanism shifted from stable nucleate boiling toward a less effective vapor-dominated regime.

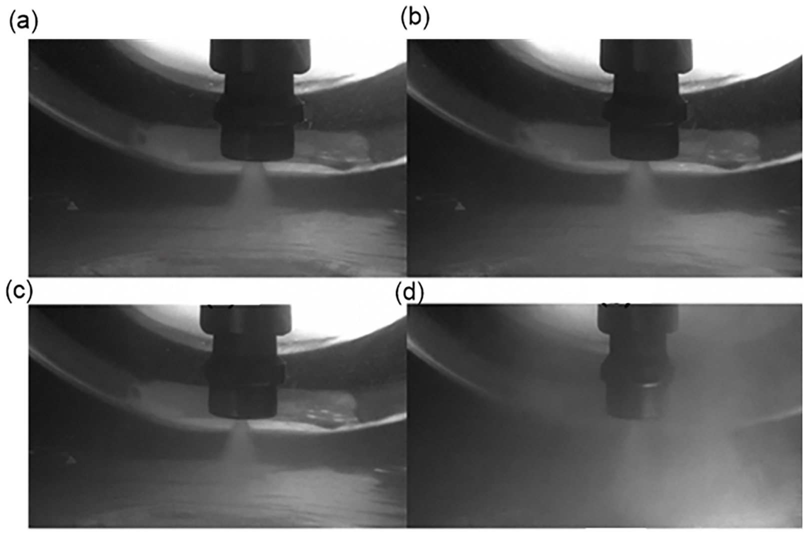

Figure 2: High-speed images of spray cooling with pure water at constant flow rate and spray height for increasing heat inputs: (**a**) 200 W—nucleate boiling, (**b**) 220 W—larger impact and vapor, (**c**) 240 W—transition boiling, (**d**) 260 W—dense vapor clouds and partial dry-out.

Overall, the images indicate that increasing thermal load gradually changed the flow condition from stable surface wetting to vapor-dominated cooling. Because only one parameter, spray height, flow rate, or heat input, was varied at a time in Table 1, the observed visual results primarily illustrate the effect of the single parameter being changed, rather than the combined influence of multiple operating conditions.

Figs. 3 and 4 also depict the effect of the flow rate and the height of the nozzle on the structure of the spray and the surface interaction at the operating conditions under which the experiment was conducted. Fig. 3 also shows a progressive change in the spray behaviour as the flow rate increases. Fig. 3a indicates that at a constant flow rate of 0.5 L/min, the spray was relatively thin and dispersed, generating a small impact area and a relatively weak surface coverage. In this case, the vapor generation was also of lesser intensity, which shows weaker droplet-surface interaction. The spray pattern in Fig. 3b turned into more uniform and wider with increasing flow rate of 0.583 L/min, which indicated a better method of atomization and spreading of the liquid on the heated surface. The slightly enhanced activity of the vapor along the impact region indicates that this increase in the droplet supply also increased the interaction between the spray and the wall.

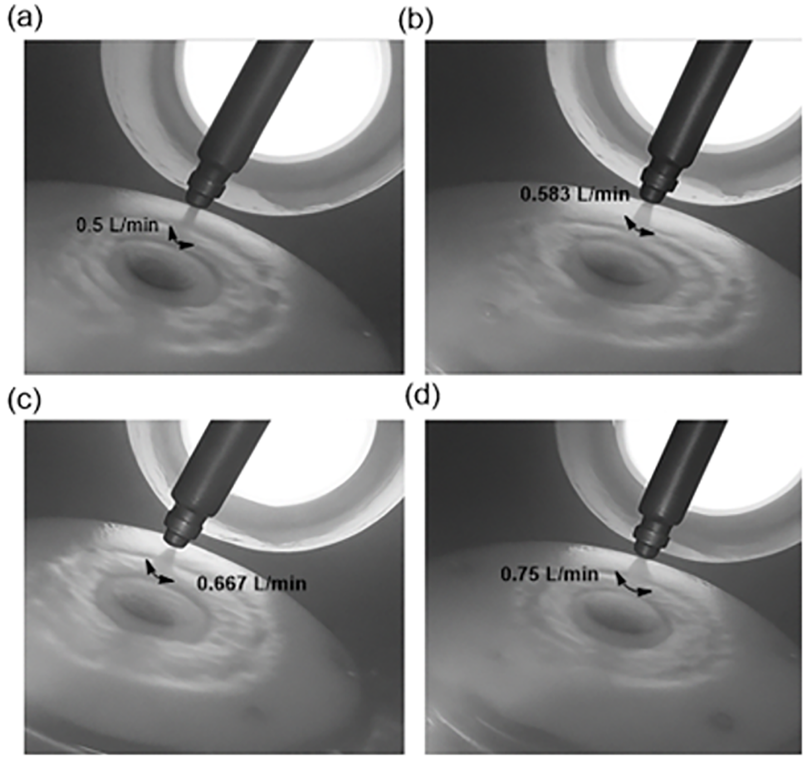

Figure 3: Spray structure formation with pure water at constant spray height for varying flow rates: (**a**) 0.5 L/min, narrow, scattered spray, (**b**) 0.583 L/min, wider spray and improved atomization, (**c**) 0.667 L/min, increased vapor formation, (**d**) 0.75 L/min, dense, well-dispersed spray with strong nucleate boiling.

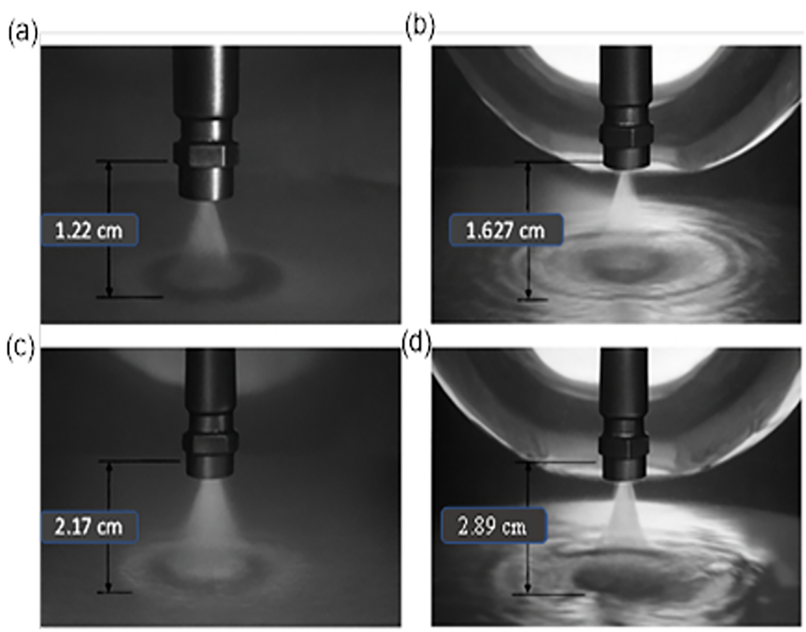

Figure 4: Spray structure formation with pure water at constant flow rate for varying nozzle heights: (**a**) 1.22 cm, concentrated spray, (**b**) 1.627 cm, broader spray, (**c**) 2.17 cm, wider cone with enhanced surface wetting, (**d**) 2.89 cm, maximum spread, improved wetting uniformity, with some vapor deposition.

A further increase to 0.667 L/min in Fig. 3c caused a more compact spray system and broader dispersion of the droplets, favouring better wetting and liquid refill. Meanwhile, the increased formation of vapour was observed, showing that the more powerful flux of droplets increased the evaporation at the surface. At the maximum flow rate of 0.75 L/min, which is depicted in Fig. 3d, the spray had the widest and most concentrated structure, offering the greatest amount of liquid supply and coverage of the greatest area compared to the cases that were tested. Nevertheless, this state was also linked to the deepest vapor activity, and it indicated that the positive effect of the improved liquid delivery was that it was complemented by the increased boiling and vapor concentration around the hot surface. Fig. 4 shows a comparable change progressively with increasing height of the nozzle. Fig. 4a demonstrates that the minimum nozzle height gave the most concentrated spray that had a comparatively small footprint, which generated intense local impingement and low lateral dispersion. With an increase in nozzle height in Fig. 4b, the spray footprint became broader, and the droplet distribution became more uniform, meaning it covered the heated surface better. Fig. 4c extended this trend with a wider spray cone, leading to enhanced wetting and enhanced contact between the droplets and the surface. The maximum nozzle height was the highest in the case of Fig. 4d, where the spray spread was broader, and more areas of the heated region had been covered by it, increasing the uniformity of wetting. However, the pictures also imply that more noticeable vapor deposition close to the surface coincided with the wider spray formation at higher nozzle heights, which may somewhat prevent persistent rewetting.

Taken together, Figs. 3 and 4 show that both increasing flow rate and increasing nozzle height enhanced spray dispersion and enlarged the wetted region on the heated surface. At the same time, both changes also intensified vapor activity near the wall, especially under the more demanding conditions. These observations indicate that cooling performance was determined by the balance between droplet spreading, liquid replenishment, and vapor accumulation. Observed changes in HTC and spray structure directly reflect the effect of the single parameter being varied under the controlled experimental conditions.

4.2 Pure-Water Cooling Response across the Tested Operating Cases

Pure water was used as the baseline working fluid to characterize the spray-cooling behaviour of the present system. Figs. 5–7 present the temporal variation of the heat-transfer coefficient (HTC) for pure water under the tested operating conditions. Overall, pure water exhibited strong cooling performance together with a relatively stable thermal response across the experimental range. In all conditions, the HTC increased rapidly following spray impingement and subsequently evolved toward a more stable regime as the interaction between the spray, liquid film, and heated surface became established.

Fig. 5 shows the pure-water response under the lower thermal-load condition. Under these conditions, the operating points associated with larger spray height and higher flow rate exhibited higher peak HTC values, consistent with improved spray dispersion, broader surface coverage, and more effective liquid replenishment. However, these differences should be interpreted within the limitations of the present operating matrix, in which spray height, flow rate, and heat input were varied individually, one parameter at a time, rather than as combined conditions.

At a heat input of 240 W, shown in Fig. 6, the operating condition corresponding to the higher spray height and flow rate produced the highest sustained HTC within the present pure-water dataset. This behaviour suggests that the operating condition provided a favourable balance between liquid supply, spray dispersion, and surface rewetting, while avoiding excessive vapor interference near the heated surface. The corresponding visualization results are also consistent with effective surface coverage and improved thermal stabilization over time.

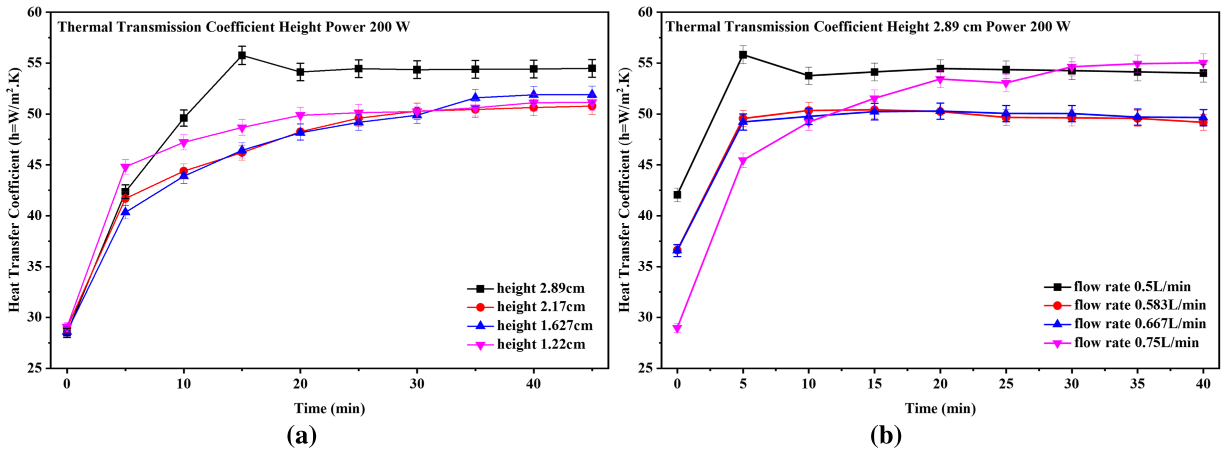

Figure 5: Heat-transfer coefficient (HTC) trends for pure water at 200 W. (**a**) Higher spray height (2.89 cm) increased peak HTC (~56 W/cm^2·K). (**b**) Higher flow rate (0.75 L/min) improved HTC (~55 W/cm^2·K).

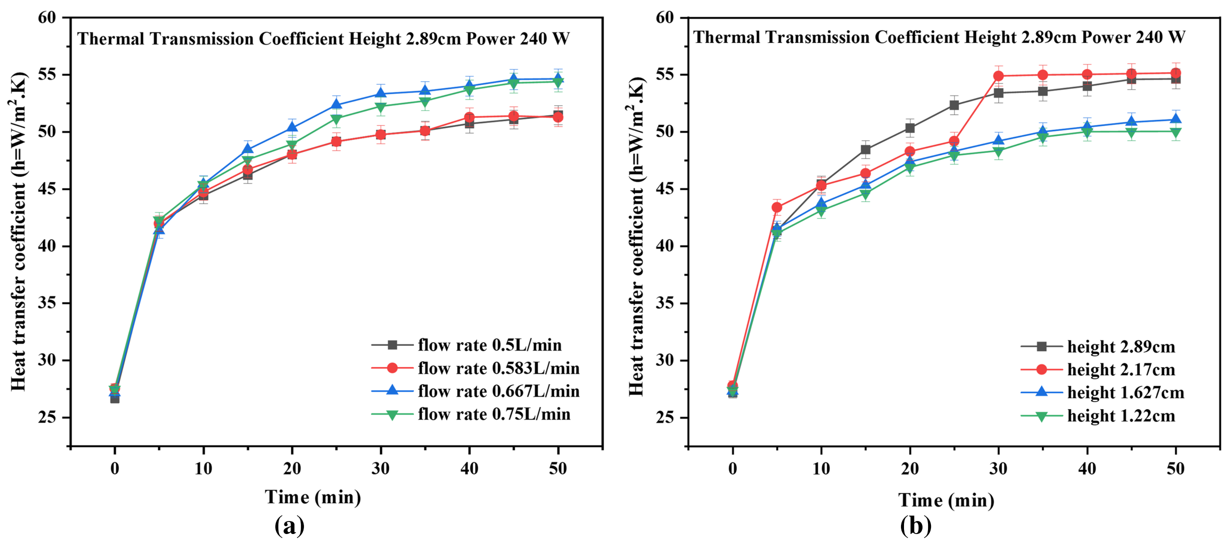

Figure 6: Heat transfer coefficient changes with time at heating power of 240 W at various heights of spray (**a**) and flow rate (**b**) in pure water.

Fig. 7 presents the pure-water response at the highest tested thermal load of 260 W. Under this condition, the operating condition associated with the largest spray height and highest flow rate still produced a strong initial HTC response; however, the subsequent HTC evolution tended to plateau relative to the strongest sustained response observed at the intermediate operating condition. This behaviour is consistent with increased vapor generation near the impact region under higher thermal loading, indicating that increased liquid supply alone was insufficient to fully suppress vapor accumulation and maintain continued HTC enhancement. These observations also confirm the interpretation that the best-performing condition in the present system reflects the influence of each individual parameter, spray atomization, liquid replenishment, or vapor management, rather than maximizing spray height or flow rate alone.

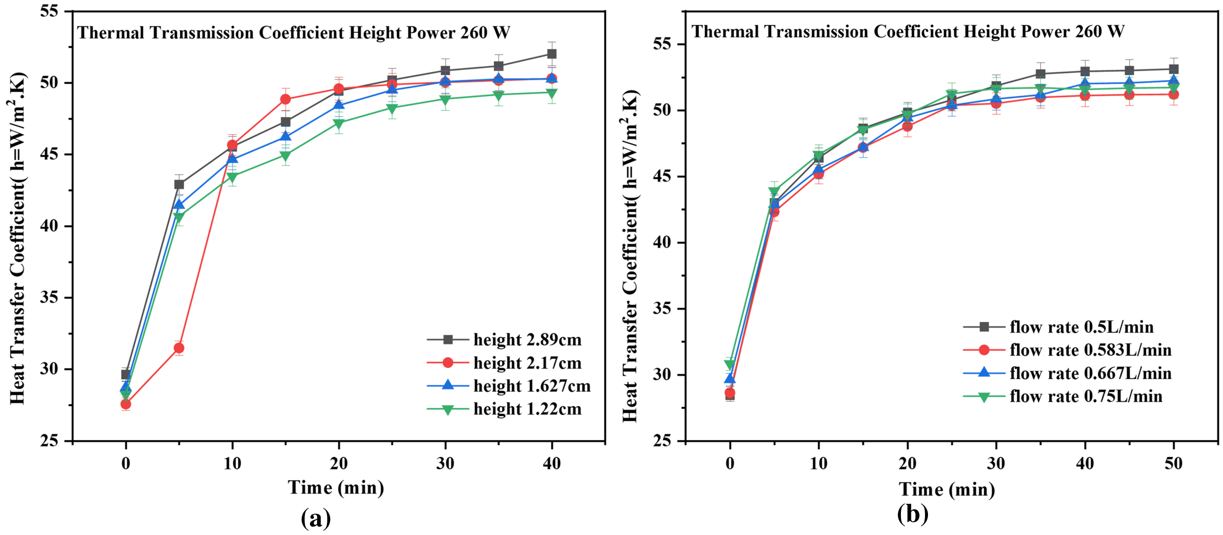

Figure 7: Time-dependent heat-transfer coefficient (HTC) for pure water at 260 W. (**a**) Variation with spray height. (**b**) Variation with flow rate. Case 4 (2.89 cm, 0.75 L/min) shows high HTC with a slight plateau.

Figs. 5–7 represent that the pure water maintained strong thermal performance across all tested conditions, with the most favourable sustained response observed for the intermediate operating condition. These results indicate that spray-cooling performance in the present system was governed by the interplay among spray dispersion, liquid replenishment, surface rewetting, and vapor removal. Within the investigated range, pure water provided a stable and high-performing reference for comparison with the low-concentration ethanol–water mixtures examined in this study.

Error bars have been included in all relevant figures to represent the estimated measurement uncertainty of the heat-transfer coefficient (HTC). Due to the limitations of the experimental setup, repeated trials for each operating condition were not performed. The error bars show uncertainties due to the instrument accuracy, flow-rate control, and temperature measurement. Although repeated measurements are not made, these estimates provide a reasonable representation of the reliability of the reported data as well as make meaningful comparisons of the cooling performance across pure water and ethanol–water mixtures.

The maximum heat-transfer coefficients (HTC) of pure water and mixtures of ethanol and water are summarized in Table 2 under the operating conditions tested. The values correspond to the maximum HTC observed for each fluid at the optimal combination of spray height (2.89 cm), flow rate (0.75 L/min), and heat input (260 W). This summary permits a direct comparison of cooling performance between fluids and highlights the non-monotonic influence of ethanol concentration on spray-cooling efficiency.

Table 2: Peak HTC values for pure water and ethanol–water mixtures at optimal conditions (2.89 cm, 0.75 L/min, 260 W).

Fluid	Spray Height (cm)	Flow Rate (L/min)	Heat Input (W)	Peak HTC (kW/m^2·K)
Pure water	2.89	0.75	260	56
2% ethanol	2.89	0.75	260	49
4% ethanol	2.89	0.75	260	48
5% ethanol	2.89	0.75	260	50

4.3 Comparative Performance of Ethanol-Water Mixtures

The ethanol–water mixtures exhibited a clear but non-monotonic concentration dependence in spray-cooling performance. Across the tested conditions shown in Figs. 8 and 9, the 5% vol ethanol mixtures consistently produced the highest HTC among the ethanol-containing fluids, followed by the 2% vol mixture, whereas the 4% vol mixture showed the weakest response. This ordering remained unchanged under both lower and higher thermal loads, indicating that the relative performance of the mixtures was robust within the present experimental window.

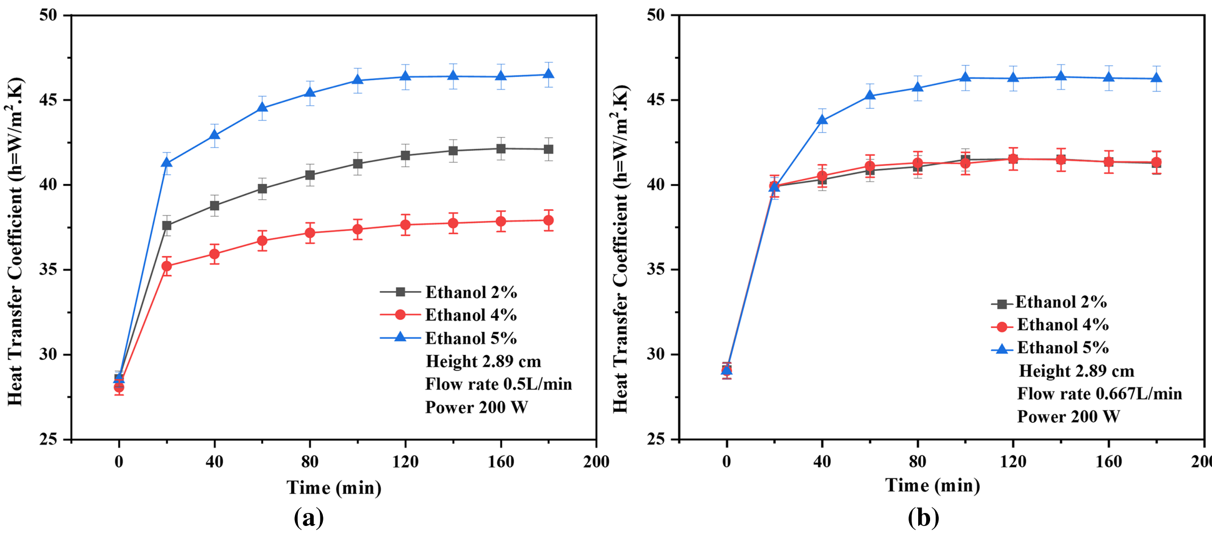

Figure 8: Heat-transfer coefficient (HTC) of ethanol–water mixtures at 2%, 4%, and 5% ethanol (vol) for 200 W power input and 2.89 cm spray height: (**a**) 0.5 L/min flow rate, (**b**) 0.667 L/min flow rate.

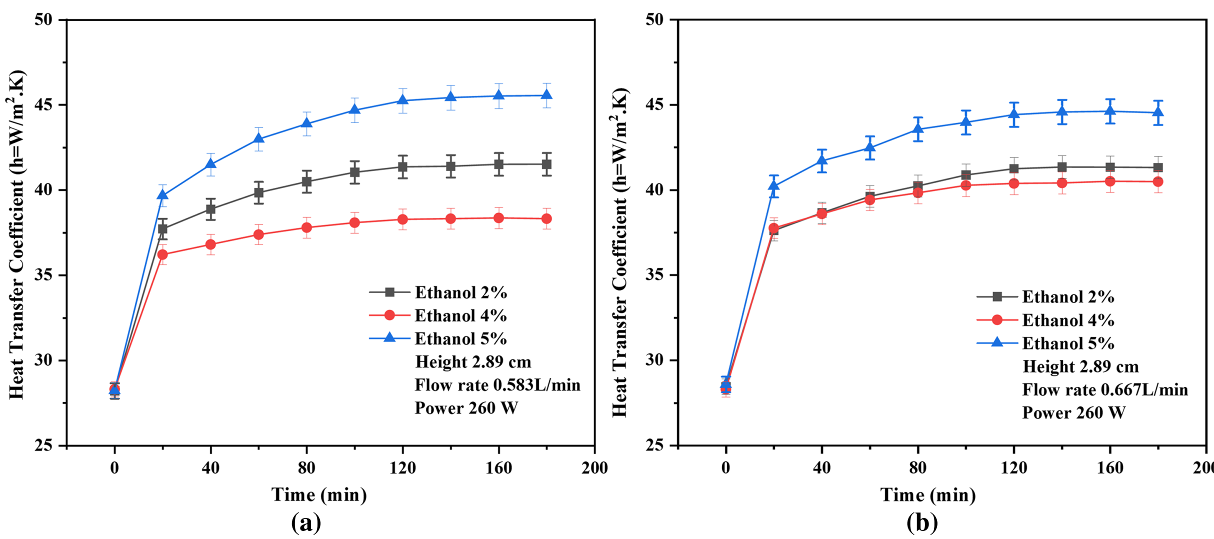

Figure 9: Dependence of the heat transfer coefficient on time of various ethanol–water combinations at the liquid height of 2.89 cm with power input of 260 W (**a**) Flow rate of 0.583 L/min (**b**) Flow rate of 0.667 L/min.

At the lower heat input of 200 W shown in Fig. 8, the same concentration ranking was observed under both tested flow-rate conditions at a spray height of 2.89 cm. When the heat input was increased to 260 W in Fig. 9, all mixtures showed a reduction in HTC, but the relative performance trend remained unchanged. In particular, among the ethanol-water mixtures tested, the 5% mixture provided the highest heat-transfer performance, whereas the 4% mixture showed a noticeable decline, especially at the lower flow condition. This behaviour suggests that the cooling response of the 4% vol mixture was more sensitive to increased thermal loading and less stable under the more demanding operating conditions.

The observed concentration dependence indicates that ethanol addition did not influence spray cooling in a simple linear manner. Instead, the results suggest the presence of competing mechanisms associated with ethanol concentration. The comparatively strong performance of the 5% vol mixture may be linked to improved atomization, enhanced droplet spreading, and better surface coverage resulting from reduced surface tension. Alternatively, the weaker response of the 4% vol mixture implies that the combined effects of wetting behaviour, liquid-film stability, vapor generation, and altered thermophysical properties were less favourable in that condition.

Despite these differences among the ethanol-containing fluids, none of the mixtures outperformed pure water. The present results therefore indicate that low-concentration ethanol addition modified the spray behaviour and altered the relative mixture response, but did not provide a net cooling advantage over the baseline fluid within the investigated range. Accordingly, the concentration ranking observed here should be interpreted as specific to the present apparatus and operating conditions rather than as a general concentration-performance hierarchy for spray-cooling systems.

4.4 Comparison between Pure Water and Ethanol-Water Mixtures

The direct comparison presented in Figs. 10 and 11 shows that pure water remained the best-performing working fluid throughout the tested thermal range. In all compared conditions, pure water produced higher HTC values than the ethanol–water mixtures, indicating that the addition of ethanol at the concentrations investigated did not provide a net enhancement in cooling performance under the present operating conditions. Among the ethanol-containing fluids, the 5% vol mixture consistently exhibited the strongest response, whereas the 2% vol and 4% vol mixtures showed lower HTC and weaker sensitivity to increasing thermal load. This performance difference is evident in Fig. 10, where pure water maintained the highest HTC across the investigated cases. Although the 5% vol ethanol mixtures approached the pure-water response more closely than the other mixtures, it remained below the pure-water baseline throughout. The 2% vol and 4% vol mixtures, by contrast, showed more limited variation with increasing heat input, suggesting a reduced capacity to sustain HTC growth as the thermal demand increased.

The same trend is reinforced by Fig. 11, which presents HTC as a function of surface temperature. Pure water showed the strongest increase in HTC with increasing surface temperature, whereas the ethanol-containing mixtures exhibited earlier saturation and, in some cases, a decline at higher temperature. This behaviour was especially evident for the 2% vol and 4% vol mixtures. The 5% vol mixture again showed the most favourable response among the ethanol-containing fluids, but still did not reach the performance level of pure water. These results suggest that, although ethanol addition may promote droplet breakup and surface spreading, such benefits were offset under the present conditions by competing effects associated with vapor accumulation, liquid-film instability, and changes in thermophysical properties at elevated temperature.

Overall, the direct water-to-mixture comparison confirms that pure water provided the highest HTC and the most favourable thermal response within the tested range, while 5% vol ethanol represented the best-performing ethanol-containing fluid. The observed ranking should therefore be interpreted as specific to the present nozzle configuration, heated surface, fluid compositions, and operating window, rather than as a universal trend for all spray-cooling systems.

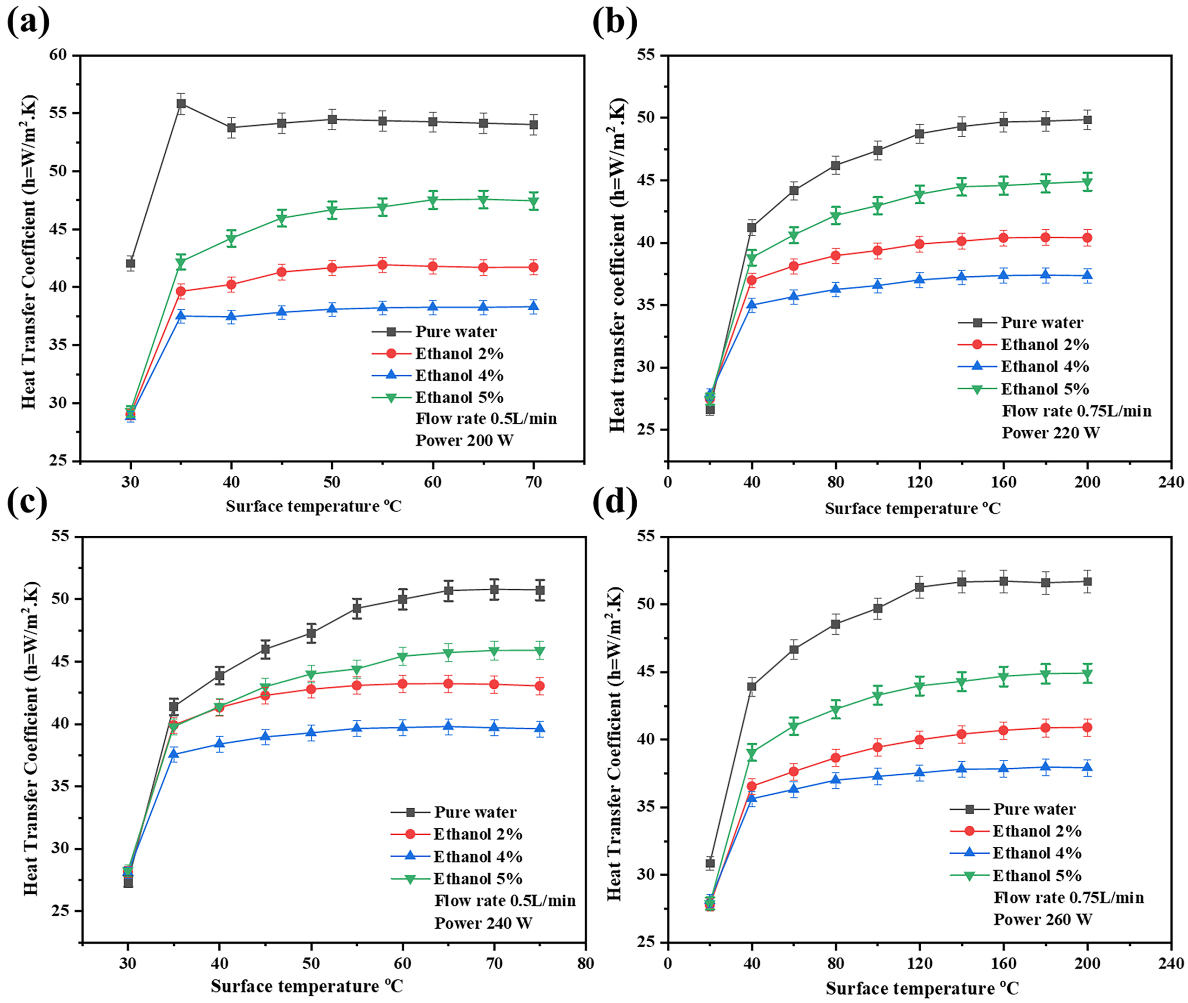

Figure 10: Heat-transfer coefficient (HTC) vs. surface temperature for ethanol–water mixtures (2%, 4%, 5%) and pure water at different power inputs and flow rates: (**a**) 200 W, 0.5 L/min; (**b**) 220 W, 0.75 L/min; (**c**) 240 W, 0.5 L/min; (**d**) 260 W, 0.75 L/min.

The trends in heat-transfer coefficient (HTC) were observed in the context of the key mechanisms of the spray cooling, namely droplet impact and spreading, liquid-film renewal, and vapor accumulation. An increase in flow rates leads to a higher liquid momentum, which results in increased droplet impact, surface spreading, and renewal of the liquid film. This minimizes thermal resistance around the wall and results in higher HTC. Similarly, higher spray height will enhance surface coverage, as more droplets are dispersed over a larger area, but excessive spray height will tend to diminish the local impact intensity, as well as partially limit heat transfer. At elevated heat fluxes, stronger vapor generation can interfere with liquid contact with the surface, reducing rewetting efficiency and causing a plateau or decrease in HTC.

The observed trends are further supported by theoretical and scaling considerations. The Reynolds number (Re) is directly proportional to the flow velocity and increases with it, enhancing inertial forces and improving droplet spreading, while the Prandtl number (Pr) reflects the impact of thermal properties of the fluid. Convective heat transfer can be approximated using Nusselt-number scaling, providing a quantitative framework for understanding the HTC enhancement at higher flow rates. These dimensionless parameters permit the trends observed in HTC to be viewed mechanistically

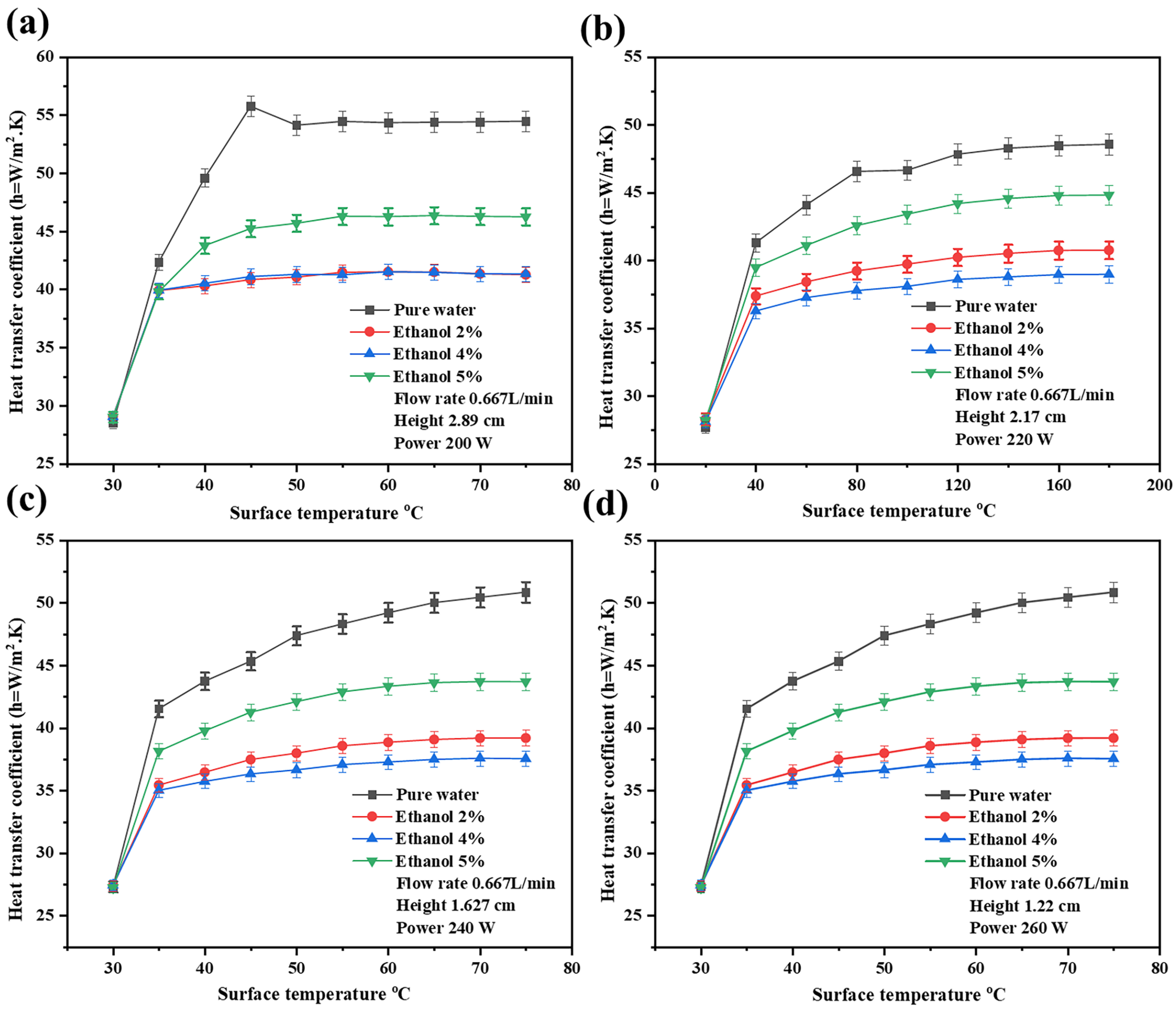

Figure 11: Heat-transfer coefficient (HTC) vs. surface temperature for pure water and ethanol–water mixtures (2%, 4%, 5%) at a fixed flow rate of 0.667 L/min. Subfigures show: (**a**) 200 W, 2.89 cm; (**b**) 220 W, 2.17 cm; (**c**) 240 W, 1.627 cm; and (**d**) 260 W, 1.22 cm. Pure water exhibits the strongest heat-transfer response, while ethanol mixtures demonstrate earlier saturation and reduced heat transfer at high temperatures.

5 Quantitative Analysis: Reynolds-Nusselt Scaling

To complement the experimental comparison of pure water and ethanol-water mixtures, a dimensionless correlation analysis was performed using the Reynolds number (Re), Prandtl number (Pr), and Nusselt number (Nu). The purpose of this section is to summarize the measured heat-transfer behaviour of the present dataset in a compact engineering form. The resulting correlation is empirical and is applicable only to the present nozzle, heated surface, working-fluid range, and operating conditions. It should therefore be interpreted as an apparatus-specific fit rather than as a universal predictive model for spray-cooling systems.

5.1 Dimensionless Groups

The Reynolds number was used to characterize the relative influence of inertial and viscous effects in the spray flow and was calculated using the nozzle diameter as the characteristic length scale. It is defined as:

$$Re = \frac{\rho_f u D}{\mu} \tag{8}$$

where ρ_f is the fluid density, u is the characteristic fluid velocity, D is the nozzle outlet diameter, and μ is the dynamic viscosity.

Qiao and Chandra [22] summarized an approximate relationship for the characteristic fluid velocity at the nozzle exit after experiments:

$$u_0 = c_q \left(\frac{2\Delta P}{\rho_f} \right)^{0.5} \tag{9}$$

Among them, c_q is the flow correction coefficient, and its value is generally between 0.6 and 1. In this study, the characteristic fluid velocity was estimated from the pressure drop across the nozzle using this flow-correction coefficient, rather than being measured directly

The dynamic viscosity of the mixed fluid is calculated by:

$$\mu_m = \left(\sum_{i=1}^{n} \varphi_i \mu_i^{\frac{1}{3}} \right)^3 \tag{10}$$

The characteristic fluid velocity for the Reynolds number calculation (Eq. (8)) was estimated using the pressure-drop method (Eq. (9)) with a flow correction coefficient ranging from 0.6–1.

The Nusselt number is a dimensionless measure of convective heat transfer relative to conductive heat transfer. The Nusselt number was determined from the experimentally calculated heat-transfer coefficient and is given by:

$$Nu = \frac{hD}{k} \tag{11}$$

where h is the heat-transfer coefficient, and k is the thermal conductivity of the working fluid.

The Prandtl number was used to describe the ratio of momentum diffusivity to thermal diffusivity. It indicates how fast momentum diffuses compared to heat within the fluid, affecting boundary layer development and heat transfer, and is given by:

$$Pr = \frac{\upsilon}{\alpha} \tag{12}$$

where υ is the kinematic viscosity and α is the thermal diffusivity.

These dimensionless groups were used to correlate the measured thermal performance of pure water and ethanol-water mixtures containing 2%, 4%, and 5% vol ethanol under the tested operating conditions.

5.2 Empirical Correlation

Based on the experimental data, a nonlinear regression analysis was performed to obtain an empirical correlation relating the Nusselt number to Reynolds number, Prandtl number, normalized spray height, and heat flux. The proposed correlation is expressed as:

$$Nu = 0.0022 \cdot Re^{0.4923} \cdot \mathrm{Pr}^{2.2144} \cdot (h/d)^{-0.0863} \cdot (q''/486725)^{0.0379} \tag{13}$$

where h is the spray height, d is the nozzle diameter, and q'' is the applied heat flux.

For the present dataset, the applicable Reynolds-number range of the correlation is 10,900–17,900, while the corresponding Prandtl-number range is 6.22–6.69. The coefficient of determination of the regression was $R^2 = 0.916$, indicating that the correlation reasonably represents the measured data within the investigated operating window.

The fitted exponents suggest that the Reynolds number had a positive influence on heat transfer in the present experiments, which is consistent with improved liquid momentum and enhanced surface replenishment at higher flow intensity. The positive exponent for the Prandtl number indicates that the thermal-diffusive properties of the working fluid also affected the cooling response. The weak negative exponent associated with normalized spray height suggests a slight reduction in the predicted heat-transfer level with increasing nozzle height within the fitted range, whereas the small positive exponent of heat flux indicates a modest increase in Nusselt number with increasing thermal load. These trends should be interpreted as empirical characteristics of the present regression model rather than as general mechanistic laws.

Fig. 12 compares the Nusselt numbers predicted by Eq. (11) with the experimental values. Most predicted values fall within approximately 7% of the measured results, indicating acceptable agreement for the present configuration. Accordingly, the proposed correlation may be used for comparative performance estimation within the tested operating range. However, because the correlation was developed for a specific nozzle geometry, smooth heated surface, fluid concentration range, and set of operating conditions, it should not be applied to other spray-cooling systems without additional validation.

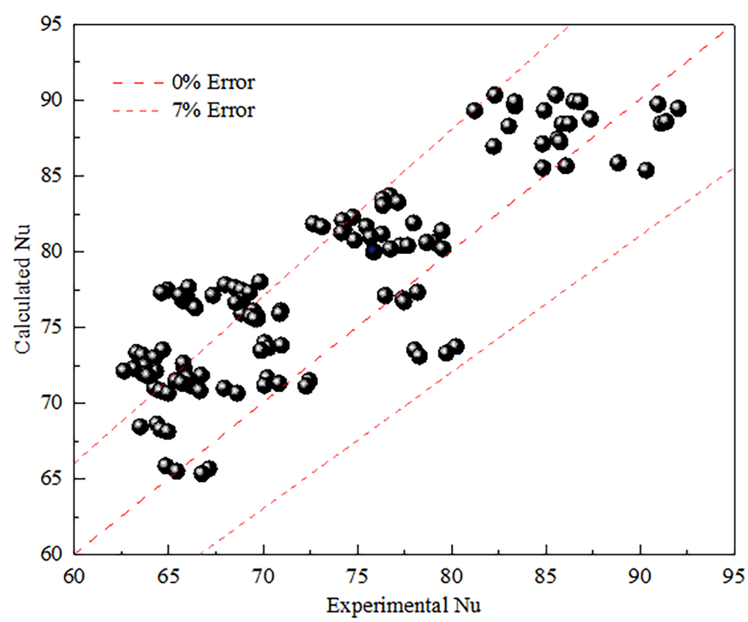

Figure 12: Comparison between experimental and predicted Nusselt numbers using the proposed empirical correlation. Most predicted values fall within approximately 7% of the experimental data, indicating reasonable agreement within the tested operating range.

The correlation provides a compact empirical representation of the present dataset and supports the experimental observations reported in Section 4. Its value lies in summarizing the relative influence of the tested variables within the current apparatus rather than in establishing a generally transferable design equation.

To provide context for the present empirical Nusselt-number correlation, with spray cooling under different additive and coverage conditions, a comparison was made with the criterion correlations reported by Niu et al. [23] for spray cooling with the use of various additives and coverage conditions. The study by Niu et.al. used the dimensionless numbers Re, Pr, and a size factor a as variables to investigate the effect of these variables on the performance of the heat-transfer process, and to determine the validity of various combinations of these dimensionless numbers. Their findings indicate that correlations considering only Re and Pr exhibited an average deviation of 38%, while the addition of a size factor α reduced the deviation to 25%, and a combined correlation incorporating Re, Pr, and α achieved the highest accuracy of ±23%. Similarly, in the present study, the proposed correlation incorporates Re, Pr, and the normalized spray height (h/d) and reproduces the experimental data within ±7%, explicitly capturing the effects of flow rate, spray height, and ethanol concentration. This comparison demonstrates that the inclusion of several dimensionless parameters, especially those that represent fluid properties, atomization, and geometric coverage, is essential for accurately predicting heat-transfer performance in spray cooling systems. The current correlation can be compared with the methodology of Niu et al., and presents a more specific apparatus-specific fit of low-concentration ethanol-water mixtures under the operating conditions explored in this work.

6 Conclusion

1. We experimentally investigated spray cooling on a smooth heated surface using pure water and ethanol–water mixtures containing 2%, 4%, and 5% ethanol under a constant spray pressure of 0.2 MPa. By systematically varying spray height, flow rate, and heat input individually, we observed non-monotonic heat-transfer behaviour and identified the mechanistic roles of droplet spreading, liquid-film stability, and vapor accumulation in determining spray-cooling performance. These findings clarify the comparative influence of low-concentration ethanol additives and provide practical guidance for designing efficient high-heat-flux thermal-management systems. The experiments were conducted in a single-nozzle system over spray heights of 1.22–2.89 cm, flow rates of 0.5–0.75 L/min, and heat inputs of 200–260 W. Cooling performance was evaluated through transient heat-transfer-coefficient (HTC) measurements together with flow visualization. Within the investigated operating range, pure water consistently provided the highest overall cooling performance and the most stable thermal response. Among the ethanol-containing mixtures, the 5% vol ethanol solutions showed the best performance, followed by the 2% vol mixture, whereas the 4% vol mixture exhibited the weakest cooling response. These results indicate that the influence of ethanol addition on spray-cooling performance was non-monotonic under the present experimental conditions.
2. The visualization results suggest that the measured thermal behaviour was governed by the interplay of droplet dispersion, surface wetting stability, liquid replenishment, and vapor accumulation near the heated surface. At higher thermal loads, increased vapor generation appeared to suppress sustained HTC enhancement, even under conditions of increased liquid supply. An empirical Nusselt-number correlation was also developed for the present apparatus and operating window. The correlation showed reasonable agreement with the experimental results, yielding an R^2 value of 0.916, with most predicted values remaining within approximately 7% of the measured data. However, this correlation should be regarded as specific to the present nozzle configuration, heated surface, working-fluid range, and test conditions.
3. Overall, this work provides a systematic investigation of low-concentration ethanol–water mixtures under controlled single-parameter variation, combining transient HTC measurements with high-speed

visualization. Unlike previous studies focusing on pure water or high-concentration additives, the present study reveals non-monotonic heat-transfer trends and mechanistic insights into how small changes in fluid composition influence droplet spreading, surface coverage, and vapor management. These contributions advance the understanding of ethanol effects in spray-cooling systems and guide the design of efficient thermal-management strategies for high-heat-flux applications.

Acknowledgement: Not applicable.

Funding Statement: The authors received no specific funding for this study.

Author Contributions: The authors confirm contribution to the paper as follows: writing—original draft preparation, Dawar Asfandyar Khan and Yanyu Chen; validation, Haokang Zhang; writing—review and editing, Yu Wang. All authors reviewed and approved the final version of the manuscript.

Availability of Data and Materials: Data available on request from the authors. The data that support the findings of this study are available from the corresponding author, Yu Wang, upon reasonable request.

Ethics Approval: Not applicable.

Conflicts of Interest: The authors declare no conflicts of interest.

References

1. Dhumal AR, Kulkarni AP, Ambhore NH. A comprehensive review on thermal management of electronic devices. J Eng Appl Sci. 2023;70(1):140. doi:10.1186/s44147-023-00309-2.
2. Ersoy K. Review of electronic cooling and thermal management in space and aerospace applications. Eng Proc. 2025;89(1):42. doi:10.3390/engproc2025089042.
3. Sapasap T, Rojas X. Reviewing cooling strategies for post-dennard era computing and modern electrothermal phenomena. J Stud Res. 2023;12(4). doi:10.47611/jsrhs.v12i4.5673.
4. Zhang Z, Wang X, Yan Y. A review of the state-of-the-art in electronic cooling. E-Prime Adv Electr Eng Electron Energy. 2021;1:100009. doi:10.1016/j.prime.2021.100009.
5. Sohel Murshed SM, de Castro Nieto CA. A critical review of traditional and emerging techniques and fluids for electronics cooling. Renew Sustain Energy Rev. 2017;78:821–33. doi:10.1016/j.rser.2017.04.112.
6. Azarifar M, Arik M, Chang JY. Liquid cooling of data centers: a necessity facing challenges. Appl Therm Eng. 2024;247:123112. doi:10.1016/j.applthermaleng.2024.123112.
7. Liang G, Mudawar I. Review of spray cooling—part 1: single-phase and nucleate boiling regimes, and critical heat flux. Int J Heat Mass Transf. 2017;115:1174–205. doi:10.1016/j.ijheatmasstransfer.2017.06.029.
8. Zhang T, Mo Z, Xu X, Liu X, Chen H, Han Z, et al. Advanced study of spray cooling: from theories to applications. Energies. 2022;15(23):9219. doi:10.3390/en15239219.
9. Mondal MTH, Alam MS, Hossain REN, Moore AL. Heat transfer and phase interface dynamics during impact and evaporation of subcooled impinging droplets on a heated surface. Appl Therm Eng. 2024;248:123152. doi:10.1016/j.applthermaleng.2024.123152.
10. Yin J, Wang S, Sang X, Zhou Z, Chen B, Thrassos P, et al. Spray cooling as a high-efficient thermal management solution: a review. Energies. 2022;15(22):8547. doi:10.3390/en15228547.
11. Vladyko I, Miskiv N, Serdyukov V, Nazarov A, Surtaev A. Influence of the Nozzle-to-surface distance on spray cooling efficiency. Fluids. 2023;8(7):191. doi:10.3390/fluids8070191.
12. Huang XZ, Li B, Zhang HL, Wang WW, Zhao FY, Cai Y. Optimizing spray cooling systems: a comprehensive study on influential parameters and their effects on heat transfer under varied heat flux conditions. Numer Heat Transf Part A Appl. 2025;86(8):2347–71. doi:10.1080/10407782.2023.2290088.

13. Chakraborty S, Shukla D, Panigrahi KP. A review on coolant selection for thermal management of electronics and implementation of multiple-criteria decision-making approach. Appl Therm Eng. 2024;245:122807. doi:10.1016/j.applthermaleng.2024.122807.
14. Cai C, Si C, Liu H, Yin H. Influence of alcohol additive and surface temperature on impact and spreading characteristics of a single water droplet. Int J Heat Mass Transf. 2021;180:121795. doi:10.1016/j.ijheatmasstransfer.2021.121795.
15. Yin H, Chen H, Cai C, Liu H, Zhao C. Spray cooling heat transfer enhancement by ethanol additive: effect of Sauter mean diameter and fluid volumetric flux. Heat Mass Transf. 2023;59(8):1459–75. doi:10.1007/s00231-023-03349-9.
16. Liu H, Cai C, Yin H, Luo J, Jia M, Gao J. Experimental investigation on heat transfer of spray cooling with the mixture of ethanol and water. Int J Therm Sci. 2018;133:62–8. doi:10.1016/j.ijthermalsci.2018.07.018.
17. Henke S, Kadlec P, Bubník Z. Physico-chemical properties of ethanol—compilation of existing data. J Food Eng. 2010;99(4):497–504. doi:10.1016/j.jfoodeng.2009.06.050.
18. Pati AR, Kumar A, Mohapatra SS. Upward and downward facing high mass flux spray cooling with additives: a novel technique to enhance the heat removal rate at high initial surface temperature. Heat Mass Transf. 2018;54(6):1669–80. doi:10.1007/s00231-017-2258-2.
19. Karpov PN, Nazarov AD, Serov AF, Terekhov VI. Evaporative cooling by a pulsed jet spray of binary ethanol-water mixture. Tech Phys Lett. 2015;41(7):668–71. doi:10.1134/s1063785015070238.
20. Bhatt NH, Lily, Raj R, Varshney P, Pati AR, Chouhan D, et al. Enhancement of heat transfer rate of high mass flux spray cooling by ethanol-water and ethanol-tween20-water solution at very high initial surface temperature. Int J Heat Mass Transf. 2017;110:330–47. doi:10.1016/j.ijheatmasstransfer.2017.02.094.
21. Moffat RJ. Describing the uncertainties in experimental results. Exp Therm Fluid Sci. 1988;1(1):3–17. doi:10.1016/0894-1777(88)90043-x.
22. Qiao YM, Chandra S. Spray cooling enhancement by addition of a surfactant. J Heat Transf. 1998;120(1):92–8. doi:10.1115/1.2830070.
23. Niu Q, Wang Y, Kang N. The influence of droplet distribution coverage and additives on the heat transfer characteristics of spray cooling under the influence of different parameters. Appl Sci. 2022;12(18):9167. doi:10.3390/app12189167.